INNOVATION WITH PURPOSE

ALLEGRO
microsystems

ANGLE ERROR CORRECTION WITH THE A33230

By Dominic Palermo
Allegro MicroSystems

ABSTRACT

The A33230 3D analog sine/cosine sensor is designed for a wide range of motor position sensing applications that require a low-latency analog signal path and externally correctable angle performance. These features are especially useful in high-speed motor control applications such as e-bikes, e-scooters, electric vehicles (EVs), and other industrial applications. Angular position can be computed easily using the two analog signals and an external processing unit. This application note describes the mathematics to convert the analog sine/cosine outputs of the A33230 into an angular position. Sensor and environmental nonidealities will impact angle accuracy; therefore, it is important to characterize the impact of these nonidealities on the sine/cosine outputs and angular position. If the sources of error are understood, the user can effectively compensate the dominant source(s) of error in a system.

INTRODUCTION

The A33230 3D sine/cosine analog output sensor is intended for magnetic position sensing applications. Each output of the A33230 is sensitive to a single axis of magnetic field, providing a linear voltage output proportional to the magnitude of the sensed field. The A33230 has two outputs, so it can sense two dimensions (i.e., any two: X-Y, X-Z, or Y-Z) of magnetic field simultaneously. Each axis is inherently orthogonal to the other, so a rotating magnetic vector in the sensitive 2-D plane will result in two orthogonal sinusoidal outputs—sine and cosine.

The sinusoidal analog outputs are eventually digitized in the system's processing unit, compensated to improve accuracy, then transformed into a single angle value. This application note focusses on:

- How to calculate an angle value from sine and cosine inputs

- How the nonidealities of the sine and cosine signals contribute to angle error

- How to improve angular accuracy via external compensation

CONTENTS

CONVERTING ANALOG SINE/COSINE INTO ANGLE

The A33230 requires a microcontroller to convert the A33230 analog sine/cosine outputs into an angle. In this case, the microcontroller must apply an algorithm to the cosine output, x, and the sine output, y, such that the angular position, Θ, can be determined. Various operations can be used to solve for Θ, such as the four-quadrant inverse tangent function $atan2(Y,X)$, a lookup table, a polynomial fit, or a coordinate rotation digital computer (CORDIC). A CORDIC calculation is commonly used when a hardware multiplier is unavailable in a simple microcontroller because it only requires addition, subtraction, bit shifting, and a lookup table. [1]

This application note assumes the four-quadrant inverse tangent function $atan2(Y,X)$ is used to calculate the angle between real vector X and real vector Y.

Native Angle

An A33230-XY-S-AR-03 is shown in Figure 1 in an end-of-shaft application to track the rotational position of a diametric magnet.
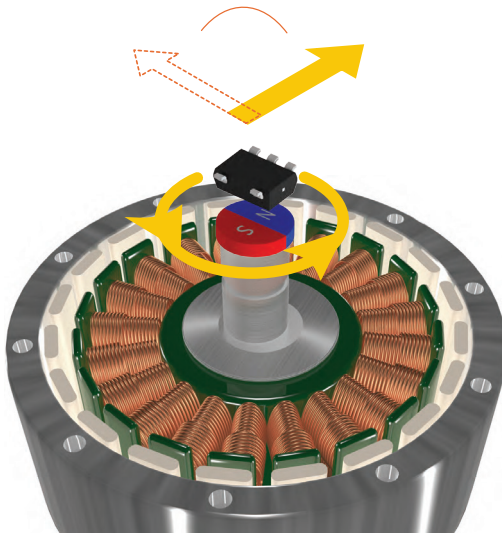

Figure 1: End-of-Shaft Rotary Position Application

For a single rotation, the analog outputs of the A33230 are recorded and plotted, as shown in Figure 2. The $atan2(Y,X)$ function [2] can be used on the sine(Θ) and cosine(Θ) signals to solve for the angle position, Θ. However, using this method alone results in significant angle error, so the signals must be normalized.
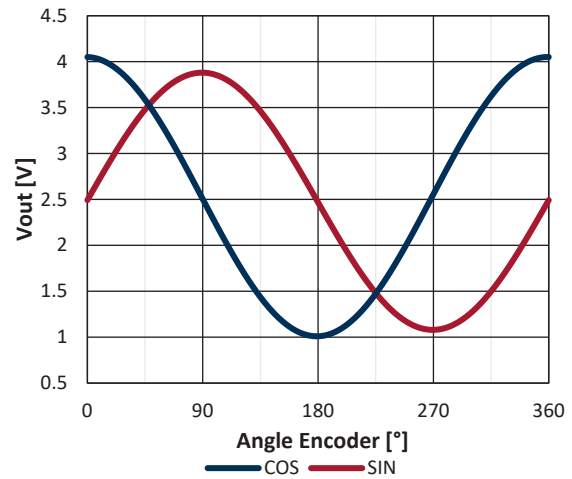

Figure 2: Native Sine/Cosine Outputs

The native angle performance can be observed if the ideal offset is blindly removed from both output signals. The A33230 has a quiescent voltage output (i.e., the output when the magnetic field is 0 G) equal to the supply voltage divided by two; therefore, with an assumed 5 V supply voltage, the ideal offset is 2.5 V. The resulting sine and cosine signals after removing the ideal offset are plotted in Figure 3.
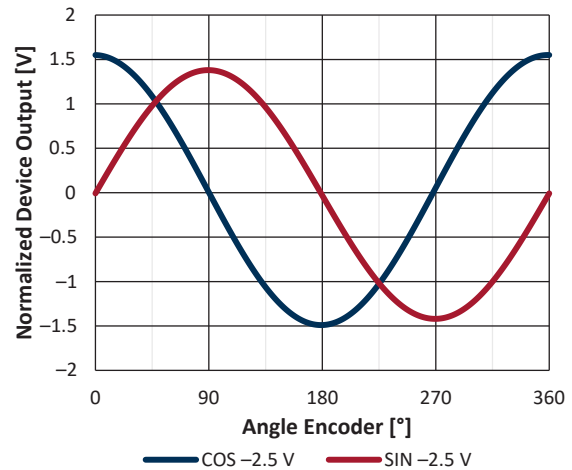

Figure 3: Output with Ideal Offset Removed

[1] Mathworks, 2008, Fixed-Point atan2 using CORDIC. Retrieved from Mathworks: https://de.mathworks.com/matlabcentral/mlc-downloads/downloads/submissions/19316/versions/2/previews/html/fixed_point_atan2_using_cordic.html

[2] The output of the atan2 function is defined between $-180° \leq \Theta \leq 180°$. The angle values discussed in this application note are shown at $0° \leq \Theta \leq 360°$; therefore, the angle values shown in this document are normalized.

The device angle, Θ_{IC}, versus the reference angle, Θ_{REF}, is shown in Figure 4. The device angle is normalized to start at the 0-degree position of the angle reference. The error between the ideal angle output and the device angle output, $\Theta_{IC} - \Theta_{REF}$, is shown in Figure 5. The maximum absolute angle error is 3.73 degrees in this example.

This error is mainly composed of offset error, amplitude mismatch, phase, and orthogonality errors in the sine and cosine signals themselves. The next section investigates each of these sources of error independently to understand their impact on the total angle error. If the contributions from each source of error can be defined, the dominant source of angle error in the system can be identified and compensations can be made to improve performance.
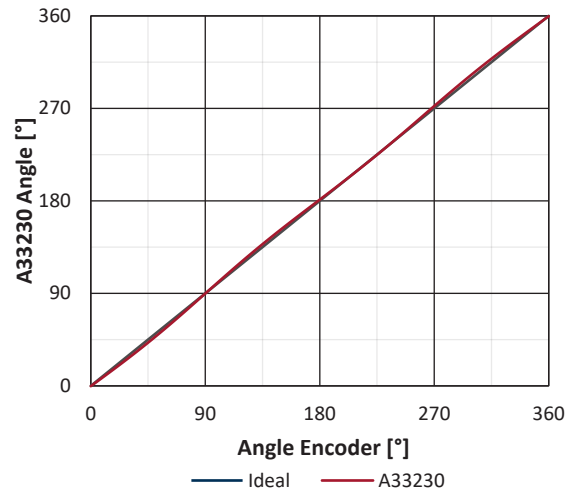

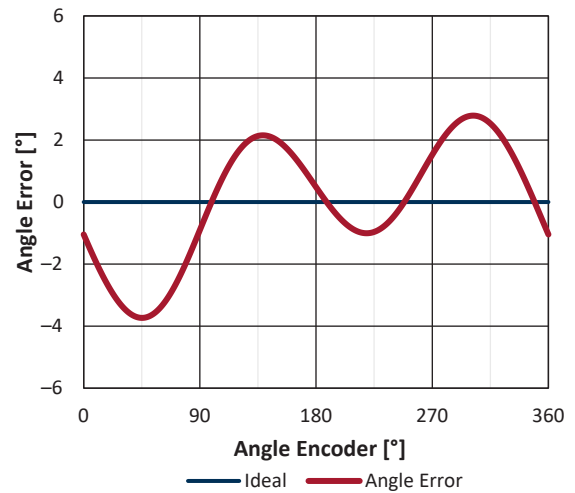Figure 4: Normalized Device Angle versus Reference Angle

Figure 5: Normalized Native Angle Error

NONIDEAL SINE/COSINE: IMPACT ON ANGLE ERROR

Output A and Output B can be described mathematically by the offset (O), amplitude (A), and phase (φ) according to:

Equation 1:

$$OUTPUTA(\Theta) = A_X \times COS(\Theta + \varphi_X) + O_X$$

$$OUTPUTB(\Theta) = A_Y \times SIN(\Theta + \varphi_Y) + O_Y$$

The offset (O) of each output is composed of the A33230 ideal offset (2.5 V) and any deviation from that ideal value (termed "offset error"). Therefore, the offset in O_X in Figure 6 includes the ideal offset of 2.5 V and the offset error.
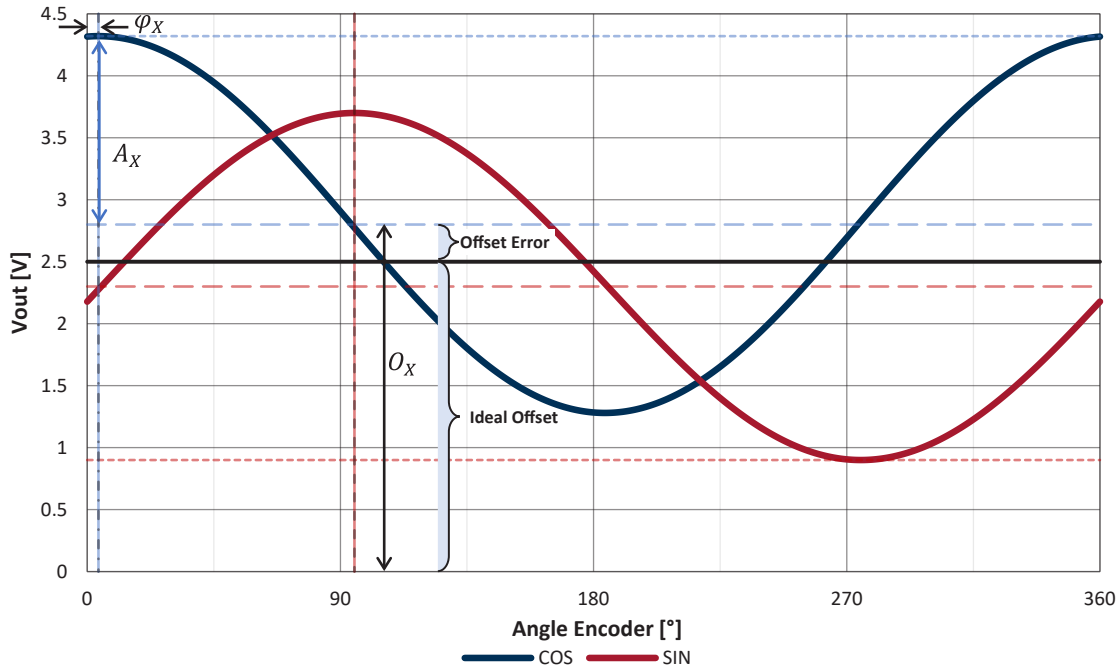

Figure 6: Understanding Offset (O), Amplitude (A), and Phase (φ)

A fast-Fourier transform can be used to solve for offset (O), first harmonic amplitude (A), and first harmonic phase (φ) as:

Equation 2:

$$fft(OUTPUTA(\Theta)) = \frac{1}{N}\sum_{n=0}^{N-1} Re(n) + i \times Im(n)$$

- $O_X = Re_{X(0)} = 2.80\ V$
- $A_X = \sqrt{Re_{X(1)}^2 + Im_{X(1)}^2} = 1.52\ V$
- $\varphi_X = atan2\left(\frac{Im_{X(1)}}{Re_{X(1)}}\right) = -4.0°$

$$OUTPUTA(\Theta) = 1.52\ V \times COS(\Theta - 4.0°) + 2.80\ V\ ;\text{ and}$$

Equation 3:

$$fft(OUTPUTB(\Theta)) = \frac{1}{N}\sum_{n=0}^{N-1} Re(n) + i \times Im(n)$$

- $O_Y = Re_{Y(0)} = 2.30\ V$
- $A_Y = \sqrt{Re_{Y(1)}^2 + Im_{Y(1)}^2} = 1.40\ V$
- $\varphi_Y = atan2\left(\frac{Im_{Y(1)}}{Re_{Y(1)}}\right) = -5.0°$

$$OUTPUTB(\Theta) = 1.40\ V \times SIN(\Theta - 5.0°) + 2.30\ V.$$

Every microcontroller digitizes these outputs differently. For simplicity, this application note describes how to solve and apply compensation in terms of the analog waveforms.

Impact of Offset on Angle Error

An ideal A33230 sensor has an offset equal to its supply voltage divided by two. Any deviation from this ideal value is considered an offset error. The impact of the offset error on the angle error is discussed here using the examples of ±10 mV, ±30 mV, ±50 mV, ±75 mV, and ±100 mV offset errors.

When the sine input has a positive offset error, there is a positive first harmonic cosine wave error with amplitude H_S. With a negative offset, the polarity of the error switches according to Equation 4, as plotted in Figure 7.

Equation 4:

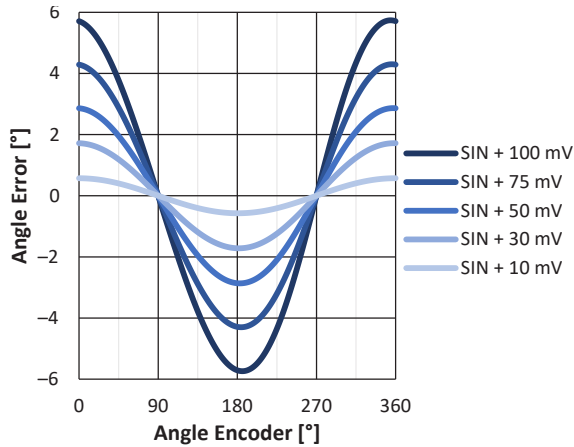$$\text{Approximation} = H_S \times COS(\Theta)$$

Figure 7: Angle Error from Sine Offset Error

When the cosine input has a positive offset error, there is a negative first harmonic sine wave error with amplitude H_C. With a negative offset, the polarity of the error switches according to Equation 5, as plotted in Figure 8.

Equation 5:
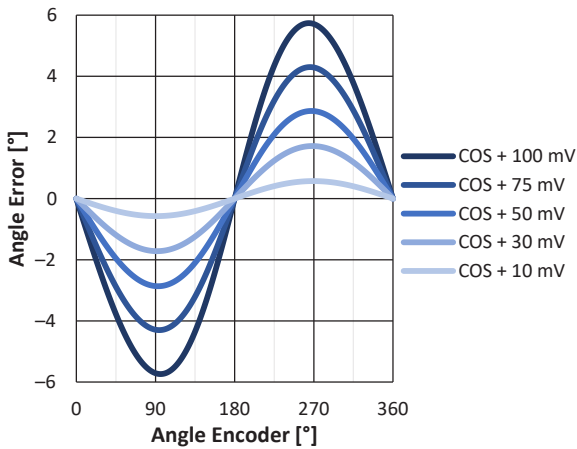
$$\text{Approximation} = H_C \times -SIN(\Theta)$$

Figure 8: Angle Error from Cosine Offset Error

When an equally positive offset is added to both inputs, there is a larger first harmonic wave error. The angle error from each input described in Equation 6 and Equation 7 are summed together and plotted in Figure 9.

Equation 6: Error from Sine Offset

$$= H_S \times COS(\Theta), where\ H_S \approx \frac{O_Y}{A_Y} \times \frac{180°}{\pi}$$

Equation 7: Error from Cosine Offset

$$= H_C \times -SIN(\Theta), where\ H_C \approx \frac{O_X}{A_X} \times \frac{180°}{\pi}$$
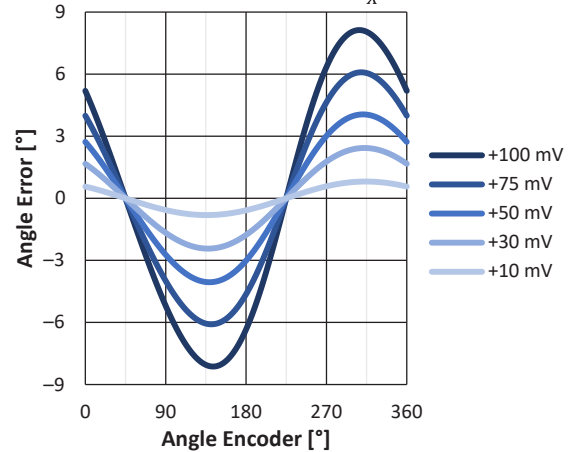

Figure 9: Angle Error from Equal Sine and Cosine Offset Error

Impact of Amplitude on Angle Error

The A33230 outputs have an amplitude proportional to the sensed magnetic field. Ideally, both outputs have equal amplitude, which implies that each signal path has a matched sensitivity and that the sensed field is uniform. This ideal situation is not a realistic scenario. The impact of amplitude mismatch on angle error is discussed here for the cases of 1%, 3%, 5%, 7.5%, and 10% amplitude mismatch.

When the sine input has a larger amplitude than the cosine input, there is a positive second harmonic sine wave error with amplitude K_S according to Equation 8, as plotted in Figure 10.

Equation 8:

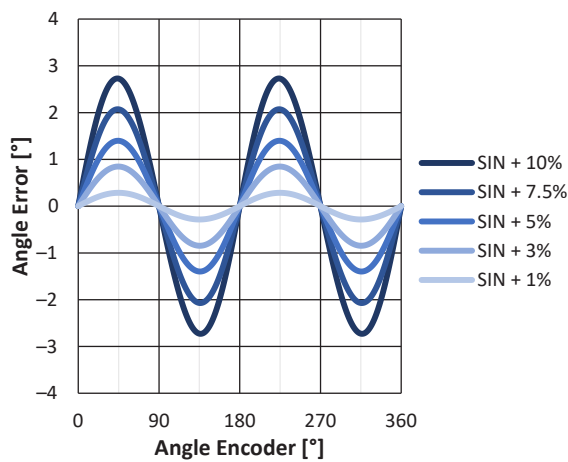$$Approximation = K_S \times SIN(2\Theta)$$

Figure 10: Angle Error from Sine Amplitude Mismatch

When the cosine input has a larger amplitude than sine, there is a negative second harmonic sine wave error with amplitude K_C according to Equation 9, as plotted in Figure 11.

Equation 9:

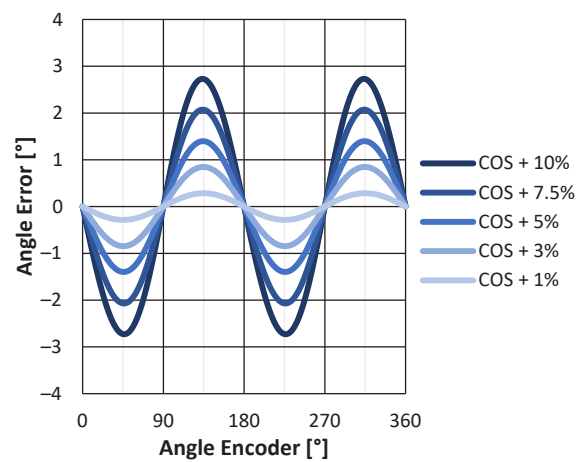$$Approximation = K_C \times -SIN(2\Theta)$$

Figure 11: Angle Error from Cosine Amplitude Mismatch

When both inputs are matched in amplitude, there is no impact to angle error. An equal change in amplitude between both inputs has the same effect as changing the magnitude of the applied magnetic field; therefore, angle error only arises from an amplitude mismatch between the inputs. Amplitude mismatch is defined in Equation 10 to be the ratio of the amplitude difference, $A_y - A_x$, to the average amplitude, A_μ. The resulting angle error is described in Equation 11.

Equation 10: Amplitude Mismatch

$$= \frac{(A_Y - A_X)}{A_\mu},$$

where $A_\mu = \frac{(A_Y + A_X)}{2}$.

Equation 11: Error Due to Amplitude Mismatch

$$\approx \frac{(180°)}{\pi} \times \frac{1}{2} \times \frac{(A_Y - A_X)}{A_\mu} \times SIN(2\Theta).$$

Impact of Phase on Angle Error

The A33230 outputs are inherently orthogonal to each other. However, nonidealities in Hall deposition and package stress can result in phase and orthogonality errors. Orthogonality error is the resulting difference between the cosine phase error, φ_X, and the sine phase error, φ_Y. This section describes the impact of phase errors of 0.2°, 0.4°, 0.6°, 1°, and 1.5° on angle error.

When the sine input has a positive phase error, there is a positive second harmonic cosine wave error with amplitude $\frac{\varphi_Y}{2}$ and offset $\frac{\varphi_Y}{2}$. With a negative phase error, the polarity of the waveform and offset switches according to Equation 12, as plotted in Figure 12.

Equation 12:

$$\text{Approximation} = \frac{\varphi_Y}{2} \times COS(2\Theta) + \frac{\varphi_Y}{2}$$
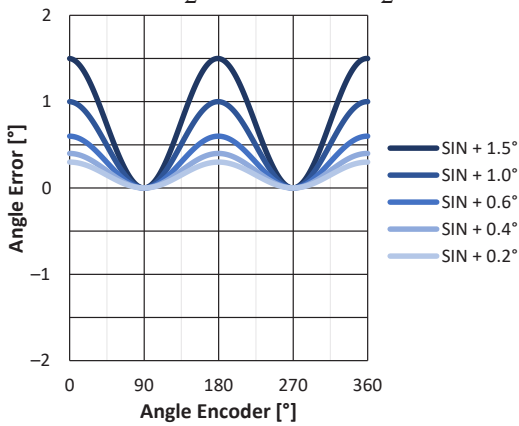

Figure 12: Angle Error from Sine Phase Error

When the cosine input has a positive phase error, there is a negative second harmonic cosine wave error with amplitude $\frac{\varphi_X}{2}$ and offset $\frac{\varphi_X}{2}$. With a negative phase error, the polarity of the waveform and offset switches according to Equation 13, as plotted in Figure 13.

Equation 13:

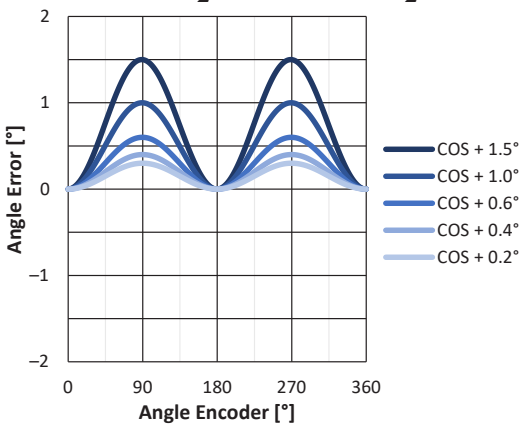$$\text{Approximation} = \frac{(-\varphi_X)}{2} \times COS(2\Theta) + \frac{\varphi_X}{2}$$

Figure 13: Angle Error from Cosine Phase Error

An equal phase error in both inputs emulates an angle shift equal to the phase error. Because Angle Error = $\Theta_{IC} - \Theta_{REF}$, when the sensor angle shifts, an offset in angle error occurs according to Equation 14, as plotted in Figure 14.

Equation 14:

Error from Sine Phase $\approx \frac{\varphi_Y}{2} \times [COS(2\Theta) + 1]$; and

Error from Cosine Phase $\approx -\frac{\varphi_X}{2} \times [COS(2\Theta) - 1]$,

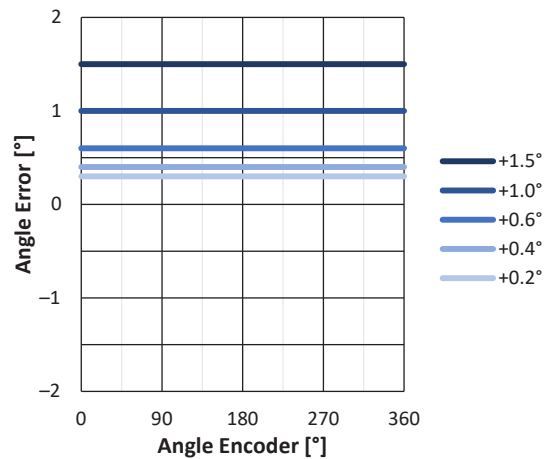where φ_X and φ_Y are in degrees.

Figure 14: Angle Error from Equal Phase Error

Approximation Summary

If the offset, amplitude, and phase components of the input sine and cosine waveforms are known, the angle error can be approximated by summing the approximations of error due to offset error, amplitude mismatch, and phase error as:

Equation 15:

- $SIN\ Offset\ Error \approx \dfrac{180°}{\pi} \times \dfrac{O_Y}{A_Y} \times COS(\Theta)$

- $COS\ Offset\ Error \approx \dfrac{180°}{\pi} \times \dfrac{O_X}{A_X} \times -SIN(\Theta)$

- $Amplitude\ Mismatch\ Error \approx \dfrac{180°}{\pi} \times \dfrac{1}{2} \times \left(\dfrac{A_Y - A_X}{A_\mu}\right) \times SIN(2\Theta),\ A_\mu = \dfrac{A_Y + A_X}{2}$

- $SIN\ Phase\ Error \approx \dfrac{\varphi_Y}{2} \times [COS(2\Theta) + 1]$

- $COS\ Phase\ Error \approx -\dfrac{\varphi_X}{2} \times [COS(2\Theta) - 1]$

$$Error\ (°) \approx \dfrac{180°}{\pi}\left[\dfrac{O_Y}{A_Y} \times COS(\Theta) - \dfrac{O_X}{A_X} \times SIN(\Theta) + \dfrac{1}{2} \times \left(\dfrac{A_Y - A_X}{A_\mu}\right) \times SIN(2\Theta)\right] \times \dfrac{\varphi_Y}{2} \times [COS(2\Theta) + 1] - \dfrac{\varphi_X}{2} \times [COS(2\Theta) - 1]$$

An approximation of error with negligible differences to the actual angle error is shown in Figure 15 for:

- $OUTPUTA(\Theta) = 1.52\ V \times COS(\Theta + 1°) + 2.53\ V$

- $OUTPUTB(\Theta) = 1.40\ V \times SIN(\Theta + 0.5°) + 2.48\ V$
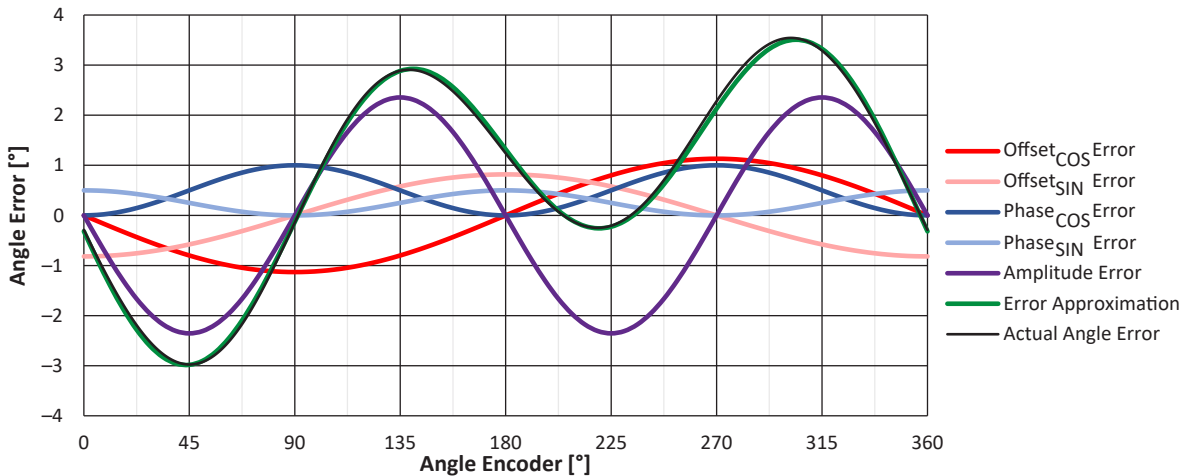

Figure 15: Approximation of Angle Error versus Actual Angle Error

EXTERNAL COMPENSATION

The angle performance can be improved by applying external compensation methods to mitigate the error due to offset, amplitude mismatch, and/or phase. This section highlights the performance improvements of: 1) blind offset correction; versus 2) one-time offset, amplitude, and phase correction; versus 3) dynamic offset and amplitude correction with a one-time phase correction. An example of both A33230 outputs at ambient temperature (T_A = 25°C) and at maximum ambient temperature (T_A = 150°C) are defined in Table 1 and plotted in Figure 16.

Table 1: Example OutputA and OutputB Signal Composition

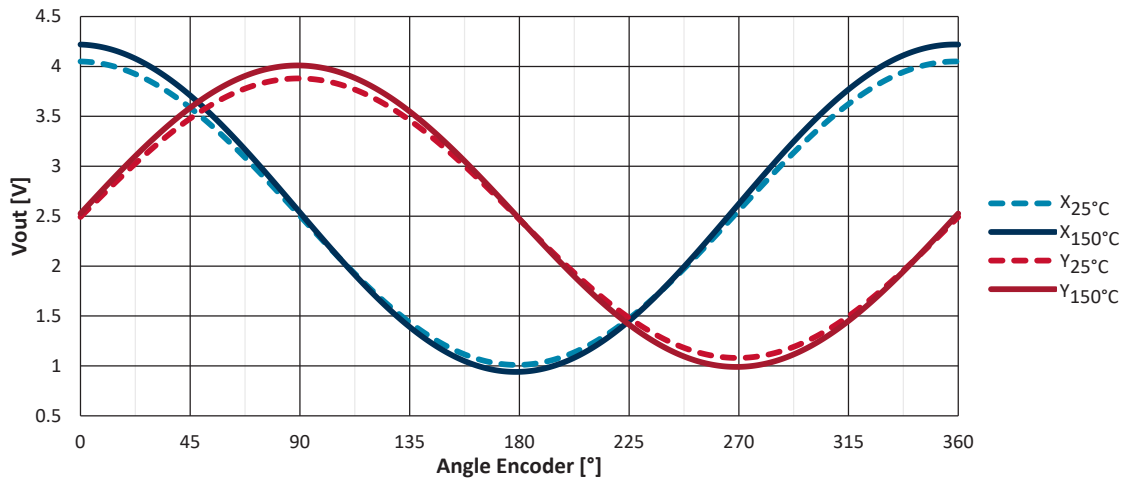| Signal	Sensing Axis	Offset (O_{TA})	Amplitude (A_{TA})	Phase (φ_{TA})
OutputA (T_A = 25°C)	X	2.53 V	1.52 V	1.0°
OutputA (T_A = 150°C)	X	2.58 V	1.64 V	1.5°
OutputB (T_A = 25°C)	Y	2.48 V	1.40 V	0.5°
OutputB (T_A = 150°C)	Y	2.50 V	1.51 V	1.0°

Figure 16: Example OutputA (X), OutputB (Y) Signals at 25°C and 150°C

Blind Offset Correction (Native Angle Error)

The resulting angle error after applying an assumed and equal offset correction to both outputs and performing the $atan2(Y_{TA}, X_{TA})$ calculation is shown in Figure 17. The assumed offset in this example is 2.5 V for all outputs because the assumed supply voltage of the A33230 is 5 V.
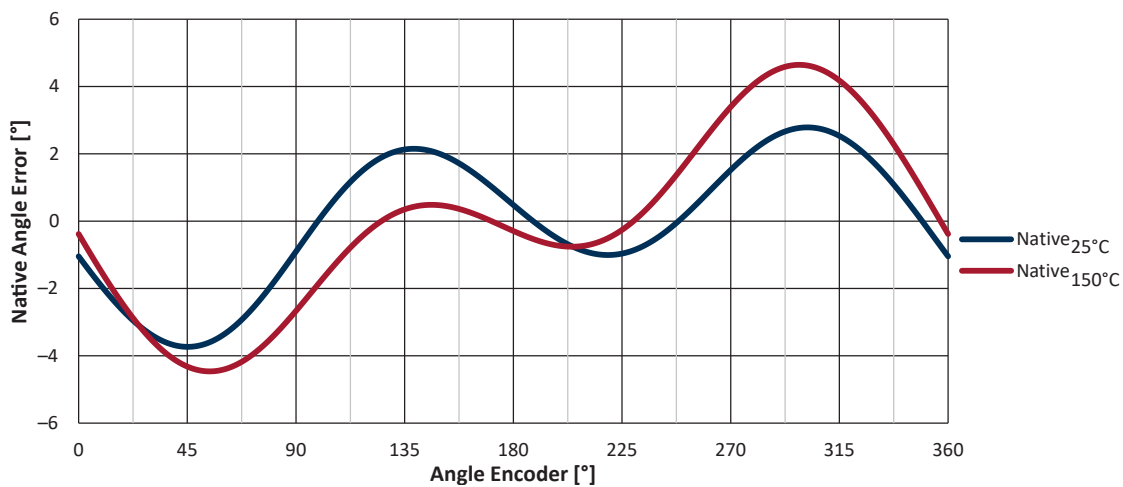

Figure 17: Angle Error After 2.5 V Offset Correction (Native Angle Error)

One-Time Offset, Amplitude, and Phase Correction

End-of-line (EOL) calibration can further improve the angle performance of the system. This section assumes the EOL calibration procedure is conducted at $T_A = 25°C$ and the offset, amplitude, and phase of both outputs are known (measured) at this temperature.

Knowns:

- $OUTPUTA(\Theta) = X(\Theta)$, $OUTPUTB(\Theta) = Y(\Theta)$

- $O_{X(TA = 25°C)}$, $O_{Y(TA = 25°C)}$, $A_{X(TA = 25°C)}$, $A_{Y(TA = 25°C)}$, $\varphi_{X(TA = 25°C)}$, and $\varphi_{Y(TA = 25°C)}$ from the EOL procedure

Unknowns:

- $O_{X(TA)}$, $O_{Y(TA)}$, $A_{X(TA)}$, $A_{Y(TA)}$, $\varphi_{X(TA)}$, and $\varphi_{Y(TA)}$ at any $T_A \neq 25°C$

Following this calibration procedure, the microcontroller blindly compensates the A33230 outputs using the correction factors solved at $T_A = 25°C$ in the following order:

1. Apply offset correction to $X(\Theta,T)$ and $Y(\Theta,T)$ at any angle, Θ, and any ambient temperature, T:

$$X_O(\Theta,T) = X(\Theta,T) - O_{X(TA = 25°C)}$$
$$Y_O(\Theta,T) = Y(\Theta,T) - O_{Y(TA = 25°C)}$$

2. Apply amplitude correction to $X_O(\Theta,T)$ and $Y_O(\Theta,T)$ at any angle, Θ, and any ambient temperature, T:

$$X_{OA}(\Theta,T) = \frac{X_O(\Theta,T)}{A_{X(TA = 25°C)}}, \quad Y_{OA}(\Theta,T) = \frac{Y_O(\Theta,T)}{A_{Y(TA = 25°C)}}$$

3. Apply phase correction to $X_{OA}(\Theta,T)$ such that X becomes orthogonal to $Y_{OA}(\Theta,T)$:

$$\Delta\varphi = \varphi_{X(TA = 25°C)} - \varphi_{Y(TA = 25°C)},$$

where $\Delta\varphi$ is the orthogonality error:

$$X_{OAP}(\Theta,T) = tan(\Delta\varphi) \times Y_{OA}(\Theta,T) + \frac{1}{COS(\Delta\varphi)} \times X_{OA}(\Theta,T)\,[3].$$

$X_{OAP}(\Theta,T)$ is now orthogonal to $Y_{OA}(\Theta,T)$.

4. Solve for an offset, amplitude, and phase-corrected angle:

$$Angle(\Theta,T) = atan2(Y_{OA}(\Theta,T),X_{OAP}(\Theta,T)) - \varphi_{Y(TA = 25°C)}.$$

Because $X_{OA}(\Theta,T)$ was phase-shifted to be orthogonal to $Y_{OA}(\Theta,T)$, the angle offset of $Angle(\Theta,T)$ will equal the phase of Y, $\varphi_{Y(TA = 25°C)}$. This angle offset can be removed simply by subtracting $\varphi_{Y(TA = 25°C)}$ from $Angle(\Theta,T)$ to align the zero-degree position of the angle reference to the zero-degree position of the device.

The progressive improvement in angle error after correcting offset ($ERR_{25°C}$, $O_{25°C}$), correcting offset and amplitude ($ERR_{25°C}$, $OA_{25°C}$), and correcting offset, amplitude, and phase ($ERR_{25°C}$, $OAP_{25°C}$) relative to a blind offset correction ($Native_{25°C}$) is shown in Figure 18. The one-time correction perfectly corrects error in the $T_A = 25°C$ dataset because the offset, amplitude, and phase are known at this temperature.
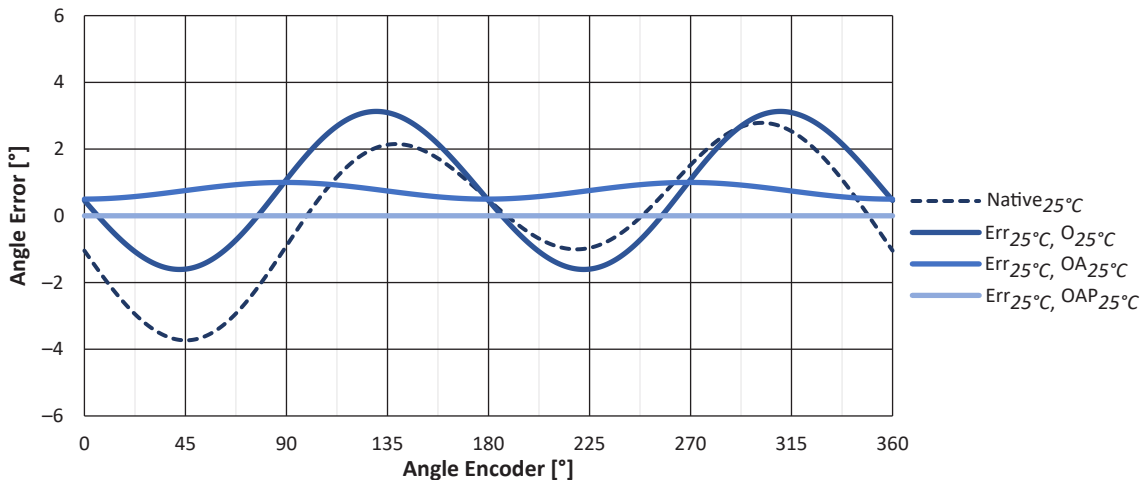

Figure 18: Native Error versus Error at 25°C after 25°C Offset, Amplitude, and Phase Correction

---

[3] Other equations/algorithms can be used in place of this equation. Regardless of the algorithm used, the procedure followed in this step is still relevant: 1) remove the orthogonality error; 2) either "zero" the reference encoder or "zero" the sine/cosine signals with an angle shift; and 3) optionally align the sensor to a known reference angle.

For all ambient temperatures outside of 25°C, the one-time offset, amplitude, and phase correction will result in residual errors. This residual error is unavoidable because the Hall elements have a temperature-dependent change in behavior. For more information about how these parameters change over temperature, refer to the A33230 datasheet. The progressive improvement in angle error after correcting offset ($Err_{150°C}$, $O_{25°C}$), correcting offset and amplitude ($Err_{150°C}$, $OA_{25°C}$), and correcting offset, amplitude, and phase ($Err_{150°C}$, $OAP_{25°C}$) relative to a blind offset correction ($Native_{150°C}$) is shown in Figure 19. Despite the residual errors after correction, there is still approximately 1.9× improvement in angle error compared to the calculation of the native angle error.
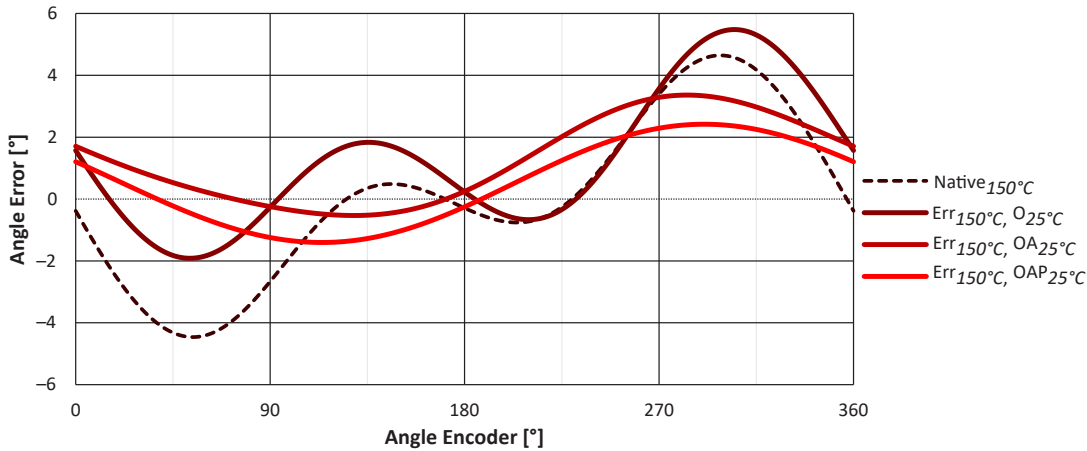

Figure 19: Native Error versus Error at 150°C after Application of 25°C Offset, Amplitude, and Phase Correction

Dynamic Offset and Amplitude Correction with One-Time Phase Correction

In addition to a one-time EOL calibration, dynamic correction of offset and amplitude can be implemented to further improve angle performance. One of the simplest methods of dynamic offset and amplitude correction is a peak-detector algorithm. The ideal maximum and minimum values of the sine and cosine signals are expressed after a rotation of at least 270 degrees. [4]

Dynamic updates of the offset and amplitude correction factors can mitigate temperature and lifetime errors. To enable these dynamic updates, the ideal maximum and minimum values of the sine and cosine values must be tracked in application.

Knowns:

- $OUTPUTA(\Theta) = X(\Theta), OUTPUTB(\Theta) = Y(\Theta)$

- $O_{X(TA = 25°C)}$, $O_{Y(TA = 25°C)}$, $A_{X(TA = 25°C)}$, $A_{Y(TA = 25°C)}$, $\varphi_{X(TA = 25°C)}$, $\varphi_{Y(TA = 25°C)}$, from the EOL procedure

- $Max(X(\Theta))$, $Min(X(\Theta))$, $Max(Y(\Theta))$, $Min(Y(\Theta))$ from the peak-detector algorithm

- $O_{X(TA)}$, $O_{Y(TA)}$, $A_{X(TA)}$, $A_{Y(TA)}$, approximated using a simple calculation

Unknowns:

- $\varphi_{X(TA)}$, $\varphi_{Y(TA)}$ at any $T_A \neq 25°C$

Recalculating Offset Using Minimum and Maximum Values:

- $O_{X(TA = T)} \dfrac{max\,(X(\Theta,T)) + min\,(X(\Theta,T))}{2}$ $O_{Y(TA = T)} \dfrac{max\,(Y(\Theta,T)) + min\,(Y(\Theta,T))}{2}$

- $A_{X(TA = T)} \dfrac{max(X(\Theta,T)) - min(X(\Theta,T))}{2}$ $A_{Y(TA = T)} \dfrac{max(Y(\Theta,T)) - min(Y(\Theta,T))}{2}$

---

[4] In a perfectly ideal environment, this is a true statement. A more robust solution should increase the minimum rotation required to ensure the maximum and minimum values were correctly sampled when considering the presence of phase errors.

The residual error after dynamically correcting offset and amplitude come from temperature-dependent phase errors, lifetime phase errors, and sampling errors. The sampling error in Figure 20 is negligible because the raw waveforms were generated in Excel with a data point every degree; therefore, the only remaining error is from phase error. The potential impact of phase error is demonstrated in Figure 21, which shows the characterized angle error performance of the A33230 after dynamic correction over temperature and over supply voltage. The plot shows the average absolute maximum performance (solid traces), plus three sigma (dashed traces) from a 180-device population composed equally from three unique wafer fabrication lots. The dynamic correction scheme in Figure 20 improves performance by approximately 9.3× relative to the blind offset correction calculation and by approximately 4.8× relative to the one-time EOL correction.
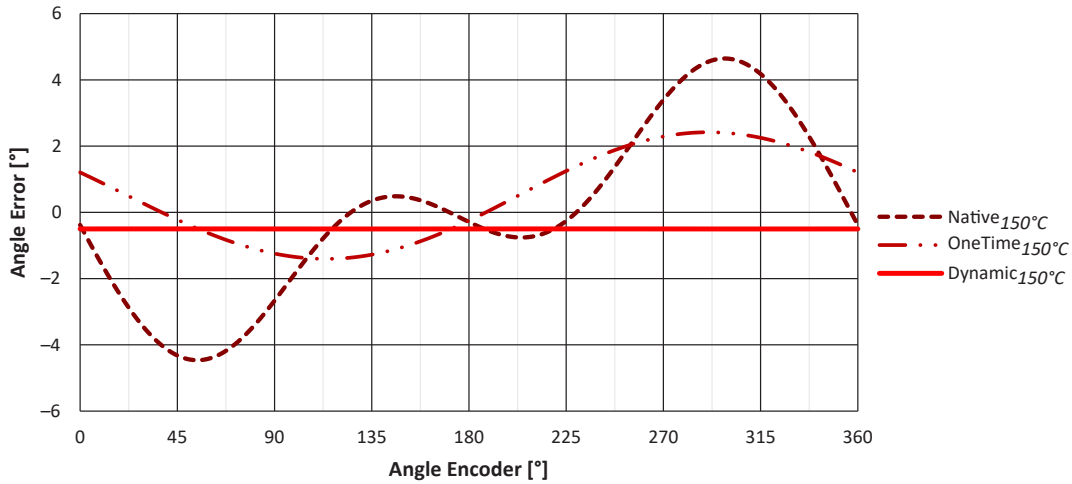

Figure 20: Comparison of Native Error, One-Time 25°C Correction Error, and Dynamic Error at 150°C
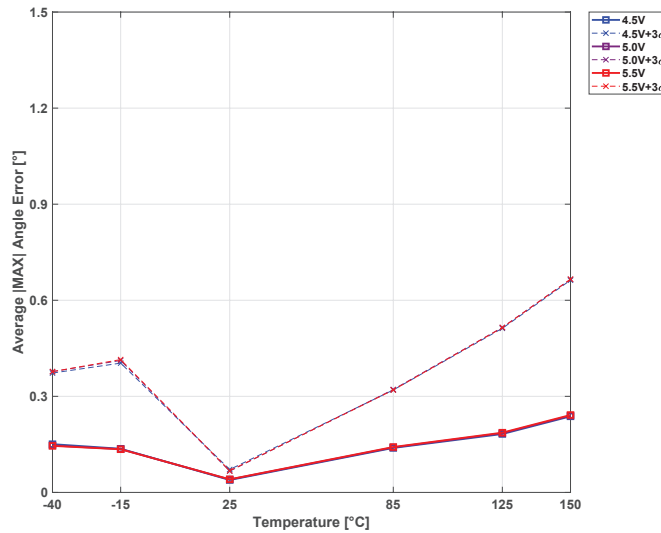

Figure 21: A33230 Average |Max| Dynamic Correction Angle Error +3σ over Temperature and Vcc

CONCLUSION/SUMMARY

The A33230 is a small, low-cost sine/cosine sensor whose performance can be greatly improved externally to fit a wide range of applications. This document, in combination with the A33230 datasheet, empowers customers to identify the dominant sources of angle error in a system, such that the most effective external correction scheme can be implemented. Some applications may prioritize speed and minimization of external computations, so the optimal solution may be to omit an end-of-line calibration and to simply perform a blind offset correction. Applications requiring higher accuracy should incorporate an EOL calibration to mitigate any sensor and system errors. In systems aiming for the highest performance, an EOL calibration and dynamic correction should be implemented. Each of these compensation methods are summarized in Table 2 below. There are other external correction techniques that could be implemented, such as using a lookup table to perform linearization, using a nonlinear-least-squares fitting algorithm for dynamic correction, or incorporating a temperature sensor to apply a dynamic temperature compensation.

Table 2: Summary of External Compensation Methods

External Compensation Method	Relative Performance	Relative Complexity	Benefits
Blind Offset	Lowest	Lowest	Fastest angle calculation No EOL calibration needed
25°C EOL	Medium	Medium	Removes sensor nonidealities at EOL ambient temperature Removes system nonidealities at EOL ambient temperature
25°C EOL + Dynamic Offset and Amplitude	Highest	Highest	Removes sensor nonidealities at EOL ambient temperature Removes system nonidealities at EOL ambient temperature Dynamically removes sensor offset and amplitude errors over temperature and lifetime Dynamically removes system offset and amplitude errors over temperature and lifetime

Revision History

Number	Date	Description	Responsibility
–	February 24, 2023	Initial release	D. Palermo

INNOVATION WITH PURPOSE

ALLEGRO
microsystems

955 PERIMETER ROAD   •   MANCHESTER, NH 03103   •   USA
+1-603-626-2300   •   FAX: +1-603-641-5336   •   ALLEGROMICRO.COM